Enabling Techniques for Optical Wireless Communication Systems

(Invited paper)

Chi-Wai Chow[1*], Chien-Hung Yeh[2], Yang Liu[3], Yinchieh Lai[1], Liang-Yu Wei[1], Chin-Wei Hsu[1], Guan-Hong Chen[1], Xin-Lan Liao[4] and Kun-Hsien Lin[4]

[1]*Department of Photonics, College of Electrical and Computer Engineering, National Chiao Tung University, Hsinchu 30010, Taiwan*
[2]*Department of Photonics, Feng Chia University, Seatwen, Taichung 40724, Taiwan*
[3]*Philips Electronics Ltd., N.T., Hong Kong*
[4]*Industrial Technology Research Institute, Taiwan*
**cwchow@faculty.nctu.edu.tw*

Abstract: We summarized the recent progress of enabling techniques for the optical wireless communication (OWC) and visible light communication (VLC). Besides, we reported two high data-rate laser-diode (LD) based VLC systems. Several application scenarios using VLC were also discussed. © 2020

OCIS codes: (060.2605) Free-space optical communication; (060.4510) Optical communications

1. Introduction

Optical wireless communication (OWC) has emerged as a complementary or alternative technology to radio-frequency (RF) communication since OWC can offer cost efficient and highly reliable access solutions for wireless communication and release the pressure on the highly congested traditional RF spectrum [1-4]. Visible light communication (VLC), a form of OWC using visible optical carrier produced by light emitting diode (LED) or laser diode (LD) has become a promising candidate for next generation wireless communication due to its advantages of long life expectancy, low power consumption, high security and using unregulated visible spectrum. Up to now, different international standard activities have already been started or completed [5], such as IEEE 802.15.7, "Short-Range Optical Wireless Communications", IEEE 802.15.13, "Multi-Gigabit/s Optical Wireless Communications", IEEE 802.11bb, "Light Communication", and ITU G.9991, "High-speed indoor visible light communication transceiver - System architecture, physical layer and data link layer specification". In the LED based VLC, one main challenge is the limited modulation bandwidth of the LED. Our team has proposed several techniques to increase its transmission data rate, such as employing hardware/software equalizers [6-9], LED nonlinearity mitigation [10, 11], advanced modulation formats [12, 13], background optical noise mitigation [14, 15]. RGB wavelength division multiplexing (WDM), polarization multiplexing, and multiple-input-and-multiple-output (MIMO) can also be employed to increase the aggregated transmission capacity [16-19]. Blue optical filter removing the slow relaxation response of the yellow phosphor to enhance the white-LED VLC data rate is usually regarded as critical; however, we modeled and illustrated by experiments that optical blue filter is not necessary in orthogonal frequency division multiplexing (OFDM) based VLC [20]. We also modeled and analyzed the influence of different indoor lamp arrangements to reduce the VLC data rate fluctuation [21]; and a real-time white-LED VLC for both illumination and communication was demonstrated [22, 23]. Recently, using the smart-phone embedded complementary-metal-oxide-semiconductor (CMOS) image sensors or camera for VLC, also known as optical camera communication (OCC) is becoming popular. However the data rate is usually limited by the camera frame rate. By employing the rolling shutter effect (RSE) of the CMOS image sensor, the VLC data rate can be higher than the frame rate [24, 25]. During the RSE operation, different pixel rows in the CMOS sensor are activated sequentially. By detecting the modulated VLC signal at the data rate higher than the frame rate, bright and dark fringes representing logic 0 and 1 can be captured in the image frame. Several synchronization and demodulation schemes for the RSE pattern were proposed and demonstrated [24-34]. Recently, we demonstrated using our developed smart-phone application programs (APP) to receive the VLC signal from display light-panel [35-38]; and this system can be applicable in places, such as restaurants, shopping malls, museums or bus stations for users to receive real-time information, such as item descriptions, or traffic conditions etc. As the Global Positioning System (GPS) does not work well for in-building environments, indoor positioning using visible light, also known as visible light positioning (VLP) is also a promising application [39, 40]. Recently, machine learning (ML) can be applied in communication to improve the transmission performance, and we employed regression techniques to enhance the accuracy in VLP [41, 42], and to enhance the decoding performance of high noise-ratio (NR) light-panel based VLC [43]. On the other hand, OWC using infrared (IR) carrier on silicon photonics (SiPh) platform for indoor access [44] or lens-free chip-to-chip communication [45] has received attentions recently. Our teams have developed several enabling SiPh devices and technologies for communication, including Franz–Keldysh vector modulator with Kramers–Kronig receiver (Rx) [46], single-side-band (SSB) modulator [47], mode-division-multiplexing (MDM) (de)multiplexer [48], etc.

Due to the decreasing cost of LD and the efficiency droop issue of LED [49], LD could be a promising candidate for solid-state lighting. LD based lighting can also provide high data rate VLC [50-54]. Here, we reported using polarization-multiplexed RGB LDs to achieve 40.7 Gbit/s VLC system with 2-m free-space transmission distance. The proposed work has potential applications for machine-to-machine (M2M) communications. We also reported using a blue LD with yellow phosphor to achieve 2.7 Gbit/s white-light VLC with 1.5-m free-space transmission distance. The luminous emission was ~500 lux, and it has potential application for indoor illustration and communication.

2. Laser-Diode (LD) based VLC Systems

Fig. 1(a) shows the experimental setup of the polarization-multiplexed RGB LD VLC system. Two arbitrary waveform generators (AWGs) at the transmitter (Tx) generated the bit-loaded and power-loaded OFDM signals for two sets of RGB LDs respectively. Fig. 1(b) shows the OFDM encoding and decoding steps implemented by using off-line Matlab® programs. The encoding process included data serial-to-parallel (S/P) conversion, symbol mapping (SM), inverse fast Fourier transform (IFFT), parallel-to-serial (P/S) conversion, and cyclic prefix (CP) insertion. The OFDM signal was applied to the LD via the digital-to-analog converter (DAC), which was the AWG. As shown in Fig. 1(a), the RGB signals at *p*-polarization and *s*-polarization were polarization multiplexed via polarization beam splitters (PBSs) and dichroic mirrors (DMs) to achieve 40.7 Gbit/s optical signal. At the Rx, photodiodes (PDs) were used to detect the optical signal, which was wavelength de-multiplexed via color filter (CF) and polarization de-multiplexed via polarizer. A real-time oscilloscope (RTO) acted as the analog-to-digital converter (ADC). The decoding process included CP removal, S/P conversion, FFT, equalization (EQ), symbol de-mapping (SDM), and P/S conversion. Figs. 1(c) and (d) show the characteristics of the LDs used, including the optical spectra, output optical power against current curves. The RGB LDs had center wavelengths of 660 nm, 514 nm and 450 nm, with full-width half-maximum (FWHM) spectral widths of ~ 2 nm. The RGB LD power conversion efficiencies were 0.91 W/A, 0.45 W/A and 0.68 W/A respectively. Figs. 1(e)-(g) show the bit-error-rate (BER) curves, which were obtained based on the measured signal-to-noise ratios (SNRs) of the OFDM subcarriers. All the wavelength and polarization de-multiplexed channels satisfied the forward-error-correction (FEC) threshold, with Rx sensitivities of 7.8 mW, 5.3 mW, and 5.7 mW for the R, G, and B signals respectively.

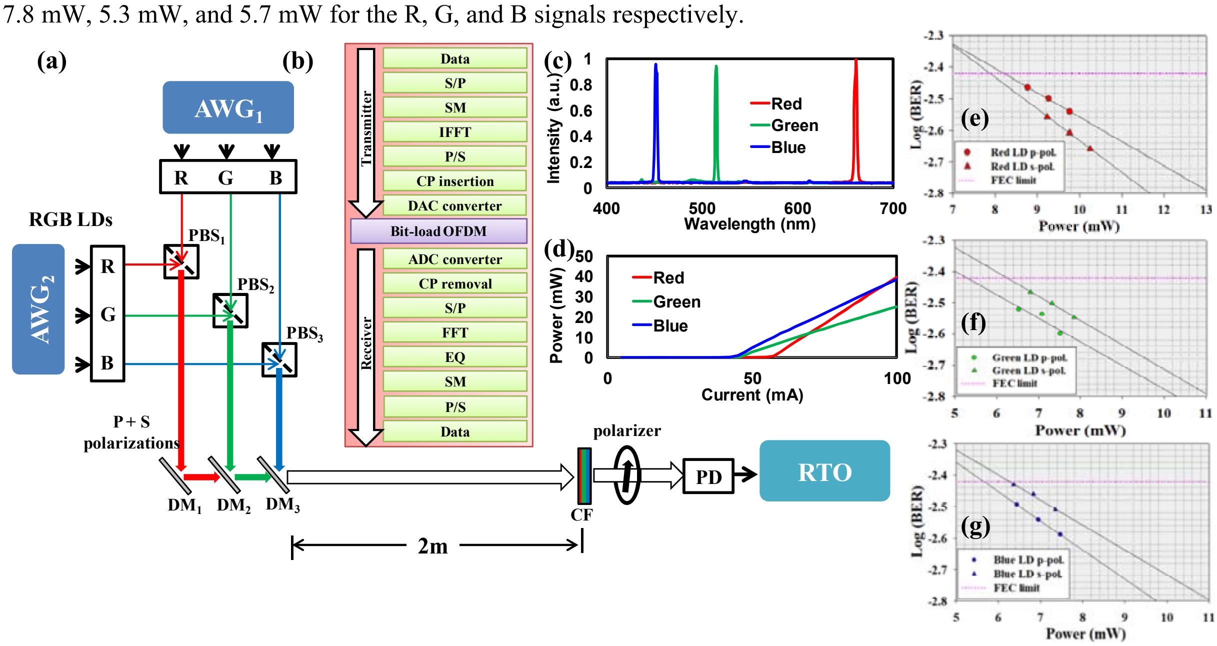

Fig. 1. (a) Experimental setup of the polarization-multiplexed tricolor RGB LD VLC system, (b) OFDM encoding and decoding steps, (c) RGB optical spectra, (d) RGB output power - current curves, (e)-(g) BER curves for the wavelength and polarization de-multiplexed channels.

Fig. 2(a) shows the experimental setup of the white-light VLC system. At the Tx, the white-light source was a blue LD + yellow phosphor. It was driven by the OFDM data. Fig. 2(b) illustrates the OFDM encoding and decoding steps, which are similar to the description for Fig. 1(b). Fig. 2(c) shows the optical spectrum of the white-light, including a 460 nm peak from the blue LD and a yellow component. Fig. 2(d) shows the 1931 CIE chromaticity coordinate, showing the white-light had a color temperature of 6000 K. After 1.5-m free-space transmission, the white-light was projected on a paper screen as shown in Fig. 2(e). It has a beam diameter of 12 cm with illuminance of ~550 lux. The measured OFDM data rate was 2.7 Gbit/s at BER of 3.2 x 10^{-3} which satisfied the FEC threshold.

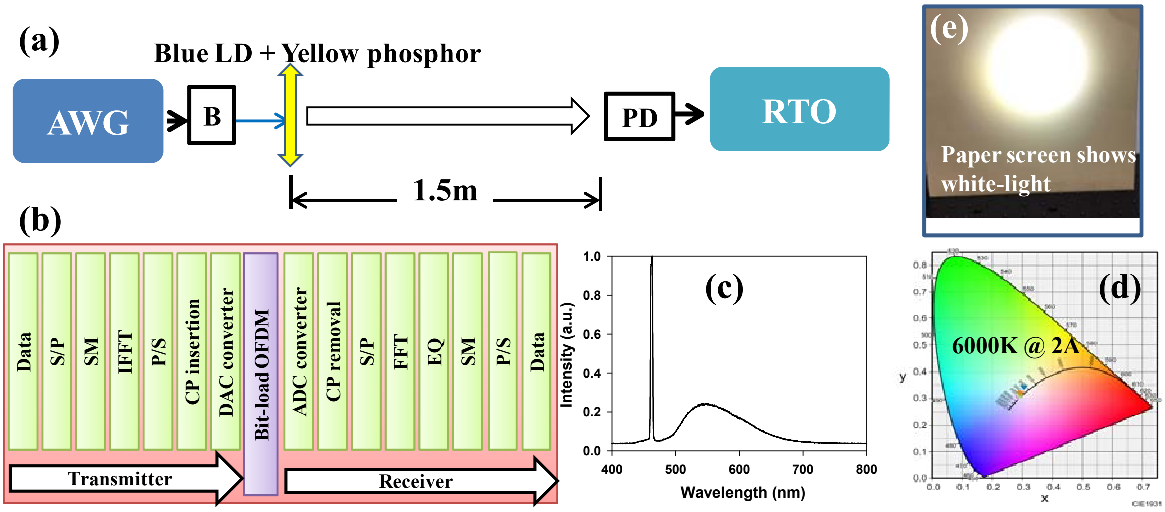

Fig. 2. (a) Experimental setup of the white-light VLC system, (b) OFDM encoding and decoding steps, (c) white-light optical spectrum, (d) CIE chromaticity coordinate, (e) white-light projection on paper screen.

3. Conclusion

We summarized the recent progress of enabling techniques for the OWC and VLC. We also reported two LD based VLC systems, including the 40.7 Gbit/s polarization-multiplexed RGB LD VLC system with 2-m free-space transmission distance, and the 2.7 Gbit/s white-light (blue LD + yellow phosphor) VLC system with 1.5-m free-space transmission distance. This work was supported by the Ministry of Science and Technology, Taiwan, ROC, MOST-107-2221-E-009-118-MY3, Higher Education Sprout Project, and Ministry of Education (MOE) in Taiwan.

4. References

[1] H. Haas, Proc. OFC 2015, Tu2G.5
[2] D. O'Brien, Proc. IEEE Summ. Top., 2016
[3] T. Koonen, Proc. ECOC 2017
[4] N. Chi, Proc. OFC 2017, Th1E.3.
[5] M. Uysal, Proc. OFC 2019, Th3I.4.
[6] C. W. Chow, et al, IEEE Photon. Soc. News., 26, 9 (2012).
[7] C. W. Chow, et al, Elect. Lett., 47, 867-868 (2011).
[8] Y. F. Liu, et al, IEEE Photon. J., 5, 7901806 (2013).
[9] C. W. Chow, et al, IEEE Access, 6, 7625 (2018).
[10] C. W. Hsu, et al, Opt. Eng., 1, 016115-016115 (2017).
[11] C. H. Yeh, et al, Opt. Exp., 23, 1133-1138 (2015).
[12] C. H. Yeh, et al, Opt. Exp., 20, 16218-16223 (2012).
[13] Y. F. Liu, et al, Opt. Exp., 20, 23019-23024 (2012).
[14] C. W. Chow, et al, IEEE Photon. J., 5, 7900709 (2013).
[15] C. W. Chow, et al, IEEE Photon. J., 5, 7900307 (2013).
[16] J. Y. Sung, et al, Opt. Exp., 22, 7538-7543 (2014).
[17] S. H. Chen, et al, IEEE Photon. J., 6, 7904106 (2014).
[18] C. H. Yen, et al, IEEE Photon. J., 4, 7904206 (2019).
[19] C. W. Hsu, et al, IEEE Photon. J., 8, 7907406 (2016).
[20] J. Y. Sung, et al, Opt. Exp., 22, 20646-20651 (2014).
[21] C. W. Chow, et al, IEEE Wireless Comm., 22, 17-23 (2015).
[22] C. H. Yeh, et al, Opt. Exp., 21, 26192-26197 (2013).
[23] C. H. Yeh, et al, Opt. Exp., 22, 9783-9788 (2014).
[24] C. W. Chow, et al, Opt. Exp., 23, 26080- 26085 (2015).
[25] C. W. Chow, et al, IEEE Photon. J., 7, 7903607 (2015).
[26] Y. Liu, et al, Opt. Exp., 24, 1973-1978 (2016).
[27] Y. Liu, et al, IEEE Photon. J., 8, 7800107 (2016).
[28] K. Liang, et al, Opt. Exp., 24, 9383-9388 (2016).
[29] K. Liang, et al, Opt. Exp., 24, 17505-17510 (2016).
[30] K. Liang, et al, Opt. Exp., 24, 25641-25646 (2016).
[31] W. C. Wang, et al, Opt. Exp., 25, 10103-10108 (2017).
[32] C. W. Chow, et al, Opt. Exp., 26, 7079-7084 (2018).
[33] C. W. Chen, et al, Opt. Exp., 25, 24362-24367 (2017).
[34] W. C. Wang, et al, IEEE Photon. J., 9, 7907606 (2017).
[35] C. W. Chow, et al, IEEE Photon. J., 10, 7902806 (2018).
[36] C. W. Chow, et al, Opt. Exp., 26, 12530 (2018).
[37] C. W. Chow, et al, Opt. Exp., 26, 22342 (2018).
[38] C. W. Chow, et al, IEEE Photon. J., 11, 7902305 (2019).
[39] C. W. Hsu, et al, IEEE Photon. J., 8, 7905507 (2016)
[40] Y. Liu, et al, Opt. Eng., 54, 120502 (2015).
[41] C. W. Hsu, et al, Proc. OFC (2018).
[42] Y. C. Chuang, et al, Opt. Exp., 27, 16377 (2019).
[43] Y. C. Chuang, et al, Opt. Exp., 27, 29924 (2019).
[44] K. Wang, et al, J. Lightw. Technol., 37, 619 (2019).
[45] C. V. Poulton, et al, Proc. FiO, paper FW5A.3., 2017.
[46] Y. Tong, et al, Opt. Lett. 43, 4333 (2018).
[47] Y. Tong, et al, IEEE Photon. J., 11, 7202108 (2019).
[48] G. H. Chen, et al, IEEE Access, 7, 129104 (2019).
[49] K. A. Denaulta, et al, AIP Advances 3, 072107 (2013).
[50] C. H. Yeh, et al, Scientific Reports, 7, 15846 (2017)
[51] L. Y. Wei, et al, IEEE Photon. J., 10, 7903407 (2018).
[52] L. Y. Wei, et al, Photon. Res., 6, 422 (2018).
[53] L. Y. Wei, et al, Proc. OFC, M3I.3 (2019).
[54] L. Y. Wei, et al, Opt. Exp., 27, 25072 (2019).